

Identification and Characterization of Phosphorus Composition in Lake Superior and St.  
Louis River Estuary Sediments Using Phosphorus Nuclear Magnetic Resonance  
Spectroscopy

A THESIS SUBMITTED TO THE FACULTY OF THE UNIVERSITY OF  
MINNESOTA BY

Hannah Schoechert

IN PARTIAL FULFILLMENT OF THE REQUIREMENTS FOR THE DEGREE OF  
MASTER OF SCIENCE CHEMICAL ENGINEERING

Dr. Guy Sander

December 2017



## ACKNOWLEDGEMENTS

This thesis has become a reality through the help of many individuals. I would like to express my sincere gratitude to all of them.

Foremost, I would like to thank my thesis committee, Dr. Guy Sander, Dr. Elizabeth Hill, and Dr. Robert Sterner, for their support, guidance, and encouragement throughout this project.

I would also like to extend gratitude to Sandra Brovold for her help and encouragement in the lab at the Large Lakes Observatory, as well as to Emily Torve and Tayler Hebner for all of their assistance.

I am highly indebted to Dr. Letitia Yao for her support and expertise in NMR spectroscopy data collection.

Many thanks and appreciations are also extended to my colleagues and people who have willingly assisted me in any capacity throughout this endeavor.

Lastly, I would like to thank my family and close friends for their constant encouragement, unwavering patience, and steadfast love over the last 2 years; without any of you, I would not have made it this far.

Funding for this project was provided by the University of Minnesota Duluth's Chancellor's Faculty Small Grant.

## ABSTRACT

Phosphorus has been a contaminant of concern for many freshwater lakes for decades. Excessive bioavailable phosphorus often leads to the eutrophication of a particular body of water. Information on the specific chemical composition of phosphorus in sediment is fundamental to understanding its bioavailability and eutrophication potential to a lake ecosystem. A single-step sodium hydroxide-ethylenediaminetetraacetic acid (NaOH-EDTA) extraction and a phosphorus nuclear magnetic resonance ( $^{31}\text{P}$  NMR) spectroscopy protocol were developed and subsequently performed on St. Louis River Estuary (SLRE) and Chequamegon Bay (CB) sediment samples. Results show the presence of phosphorus-containing compounds comparable to other oligotrophic waterbodies, and compounds typically detected in sediment samples from eutrophic lakes were not detected in any sample. For the CB samples, as the water depth increased, so did the number of peaks identified. Similarly, as the number of peaks increased, there was an increase in relative abundance of different phosphorus. For the SLRE samples, it was observed that the phosphorus composition in the sediment mirrored the phosphorus sediment composition from the Chequamegon Bay samples, suggesting there are similar hydrological conditions between the two sites.

# TABLE OF CONTENTS

<b>Acknowledgements</b>	<b>i</b>
<b>Abstract</b>	<b>ii</b>
<b>List of Tables</b>	<b>iv</b>
<b>List of Figures</b>	<b>v</b>
<b>List of Abbreviations</b>	<b>vi</b>
<b>Background</b>	<b>1</b>
<i>Introduction</i>	<i>1</i>
<i>Location Selection</i>	<i>3</i>
<i>Phosphorus Sediment Interactions</i>	<i>5</i>
<b>Methods</b>	<b>7</b>
<i>Sediment Extraction Procedure</i>	<i>7</i>
<sup>31</sup> P NMR Preparation	<i>8</i>
<sup>31</sup> P NMR Acquisition Protocol	<i>8</i>
<b>Results and Discussion</b>	<b>10</b>
<sup>31</sup> P NMR Optimization Study	<i>10</i>
<i>Spectral Results and Discussion</i>	<i>12</i>
Lake Superior Chequamegon Bay Sediment Samples	<i>12</i>
St. Louis River Estuary Sediment Samples	<i>14</i>
<i>Literature Comparisons</i>	<i>15</i>
<b>Conclusions</b>	<b>16</b>
<b>Future Work</b>	<b>17</b>
<b>Illustrations</b>	<b>20</b>
<b>Bibliography</b>	<b>29</b>

## LIST OF TABLES

<i>Table 1: Water depths for Chequamegon Bay sampling locations.</i>	21
<i>Table 2: Water depths for St. Louis River Estuary sample sites.</i>	22
<i>Table 3: Chequamegon Bay phosphorus compound identification based on <math>\pm 0.5</math> ppm from measured NMR peak.</i>	26
<i>Table 4: Summary of observed <math>^{31}\text{P}</math> NMR peaks for CB samples compared to site depth.</i>	27

# LIST OF FIGURES

<i>Figure 1: Lake Erie algal bloom captured on July 28, 2015 by the Operational Land Imager on Landsat 8. (Image courteous of NASA) .....</i>	<i>20</i>
<i>Figure 2: Aerial view of Lake Superior with sampling sites shown in boxes. Lake Superior CB sample location is outlined in blue and SLRE sample location is outlined in yellow See Figures 3 and 4, respectively, for more detail. ....</i>	<i>20</i>
<i>Figure 3: Chequamegon Bay sediment sample locations. Image was generated using Google Earth.....</i>	<i>21</i>
<i>Figure 4: St. Louis River Estuary sediment sample locations. Image generated using Google Earth.....</i>	<i>22</i>
<i>Figure 5: Sample CB12 collected with Bruker default <sup>31</sup>P NMR protocol with increasing number of scans. As the number of scans increased, the spectral resolution also increased. ....</i>	<i>23</i>
<i>Figure 6: Sample CB12 collected at 90° pulse width for 5000 scans for AQ/D1 of 3 seconds (middle) and AQ/D1 of 5 seconds (bottom), with spectral difference between the two displayed on top.....</i>	<i>23</i>
<i>Figure 7: Sample CB12 collected with three different pulse widths, 90° (top), 45° (middle), and 30° (bottom). Comparison of these three pulse widths shows the 90° having the greatest distinction between two neighboring peaks. ....</i>	<i>24</i>
<i>Figure 8: Overlay of <sup>31</sup>P NMR spectra for Chequamegon Bay Sediment Samples. ....</i>	<i>25</i>
<i>Figure 9: Relative abundances of phosphorus fractionations for select sediment cores. ....</i>	<i>27</i>
<i>Figure 10: Overlay of <sup>31</sup>P NMR spectra for St. Louis River Estuary Sediment Samples.....</i>	<i>28</i>

## LIST OF ABBREVIATIONS

---

$^{31}\text{P}$	Phosphorus
ATP	Adenosine triphosphate
AQ/D1	Acquisition time plus pulse delay time
CB	Chequamegon Bay
D <sub>2</sub> O	Deuterium oxide
EDTA	Ethylenediaminetetraacetic acid
LLO	Large Lakes Observatory
NaOH	Sodium Hydroxide
NMR	Nuclear Magnetic Resonance
RF	Radio Frequency
S/N	Signal-to-Noise
SLRE	St. Louis River Estuary



# BACKGROUND

## INTRODUCTION

Commonly referred to as the “most essential of nutrients,” phosphorus is the basis for building biomass, and is frequently present in low concentrations in surface waters due to the low solubility of phosphorus-bearing minerals [1,2]. Phosphorus loading often dictates the trophic status of freshwater lakes, since it is directly related to the rate or intensity of primary production [3–6]. While nitrogen can be fixed from the atmosphere by nitrogen-fixing bacteria, phosphorus can only enter waterways from external sources [7]. In the 1950s and 1960s, phosphorus-based products were highly popular in the developed world and entered the Great Lakes through direct discharge, agricultural runoff, and inadequately treated sewage effluents [3].

Over centuries, most lakes naturally transition from an oligotrophic waterbody, characterized by low biological productivity, low algal concentrations, and intense water clarity, to a eutrophic waterbody that exhibits high biological activity [1]. Phosphorus-rich effluents, like the ones mentioned above, increase the natural rate at which a waterbody receives phosphorus and other nutrients, and are known to cause lakes to reach eutrophic status in as little as two decades [8,9]. The over-enrichment of freshwater aquatic systems and the subsequent degradation of water quality by anthropogenic sources, which has been referred to as cultural eutrophication, has resulted in the one of the most visible examples of human changes to aquatic systems across the globe [8,10,11]. Consequences of cultural eutrophication include increased biomass of

phytoplankton and macrophyte vegetation, dissolved oxygen depletion, and drinking water treatment problems [12].

In 1972 the Clean Water Act was passed by the Congress of the United States, and simultaneously, Canada and the United States signed the Great Lakes Water Quality Agreement, aimed at improving water quality through phosphorus load reduction efforts [13]. Advancements were made to the processing of industrial and municipal pollution discharges and the use of phosphorus-based products was drastically reduced. As a result, there was a decrease in the phosphorus input levels and a decrease in phosphorus levels in the water column [14]. Primary production levels responded accordingly, even in the most impacted of lakes [15], and water quality began to improve throughout the 1980s; however, there began a secondary increase in water quality impairments [16]. For example, the annual external phosphorus loading level for Lake Erie was reduced to 11,000 metric tons in 1978 [16]. Water quality in Lake Erie began to improve through the 1990's; however, an image captured of western Lake Erie (Figure 1) in 2015 shows that massive algal blooms are still occurring.

In addition to being a nuisance to those proximal to the lake, large algal blooms can also affect local and regional economies. In a record-breaking algal bloom in 2011 that covered approximately 5,000 km<sup>2</sup>, Lake Erie had estimated levels of microcystin toxin upwards of 4,500 µg/L at the surface [17]. Though blooms of this magnitude do not occur annually, Lake Erie still experiences large-scale blooms that often clog industrial water intake systems, require additional water treatment, and adversely impact commercial fishing activities, as well as degrade aquatic habitats and populations [16]. Additionally, the Lake Erie Ecosystem Priority report serves as an illustrative order-of-

magnitude comparison and estimated that large algal blooms had an economic impact on several industries for Ohio. The report estimated that housing values could be affected at distances up to 10 miles inland due to the negative aesthetics of these large blooms. Similarly, the economic value of damages to recreation fishing and beach recreation (for Maumee Bay State Park) were estimated to be \$2.4 million and \$1.3 million, respectively [18].

## LOCATION SELECTION

Even though Lake Erie continues to experience the greatest effects of excessive phosphorus concentrations relative to the other Great Lakes, it is of importance to study and understand the consequences of over-enrichment in Lake Superior. Phosphorus-poor in comparison to other aquatic systems, Lake Superior receives approximately 70% of its annual phosphorus load through rivers, 20% through the atmosphere, and the remainder through municipal and other sources [19]. Lake Superior is of importance because it is the deepest of all of the Great Lakes and currently exhibits the least amount of eutrophication, as evident by its clean water, low biological activity, and high oxygen conditions at the sediment-water interface [19,20]; however, in recent years, blue-green algae has been spotted along the shores of the Apostle Islands [21], increasing the need to study the bioavailability and eutrophication potential of phosphorus.

Based on hydraulic retention time, a portion of phosphorus is retained in the sediment under steady-state conditions [12]. Phosphorus retention has often been observed to have seasonal variation between summer and winter, where summer water phosphorus levels can exceed those measured in the winter by 200-300% in shallow lakes [12,22], suggesting a strong seasonal dependence on the release of phosphorus from the

sediment. Although other factors also change between the summer and winter seasons, one significant variable is temperature. Lake Superior is the coldest of the Great Lakes, over the last century the surface water temperature has increased 3.5°C with most of the warming occurring in the last three years studied [23]. This increase in water temperature is significantly greater than the rate of increase in regional atmospheric temperatures [23–25].

Since sediment retention decreases with increasing water temperatures, having a water body that is experiencing increasing average water temperatures brings studying Lake Superior into more focus to better understand sediment-phosphorus interactions. Specifically, researchers at the Large Lakes Observatory (LLO) have been studying total water phosphorus, total sediment phosphorus, and phosphorus fractionations to better understand these delicate interactions. Samples for this investigation were provided by LLO and were selected based on previous work alignment [26]. Figure 2 shows the areas on Lake Superior from which the Chequamegon Bay (CB) and the St. Louis River Estuary (SLRE) samples were taken.

As shown in Figure 3, the CB samples were clustered around the eastern side of the Apostle Islands, with samples CB3 and CB4 taken from the same core location. Sample CB3 was collected from core depth 0-1cm, and sample CB4 was collected at core depth 1-2cm from the sediment-water interface. Sediment samples from CB3, CB4, and CB12 were observed to be brown to dark-brown in color with a fine, powdery consistency, whereas samples CB10 and CB11 were lighter in color and had larger particle sizes, much more comparable to fine sand.

St. Louis River Estuary samples were taken at several points within the estuary, starting at the Oliver Bridge (SLRE 2) and ending in the Allouez Bay (SLRE 10), as shown in Figure 4. Similar to some of the Chequamegon Bay samples, all SLRE sediment samples were observed as brown to dark-brown in color with a fine, powdery consistency. Table 1 and Table 2 have water depths for CB and SLRE sample locations, respectively.

### PHOSPHORUS SEDIMENT INTERACTIONS

Phosphorus that accumulated in sediment during high loading periods needs time to reach equilibrium with the water column at the current loading level [12]. After a reduction in loading occurs, two processes control the internal loading of phosphorus: (i) the downward flux caused mainly by sediment deposition and (ii) the upward flux, or gross release, of phosphorus driven by the decomposition of organic matter, phosphorus gradients, and transport mechanisms in the sediment. Internal loading of phosphorus from sediment into the water column, where it becomes biologically available for uptake by microorganisms, has now become one of the primary factors in determining the trophic status of a lake [12,27–29]. Internal loading of phosphorus may be so great and persistent that it may prevent total improvement in water quality [12,30,31].

Phosphorus release is a function of the quantity and distribution of phosphorus fractions within the sediments, the degree of saturation of exchangeable phosphorus, and the hydrological conditions [32–35]. Information on the specific chemical composition of phosphorus in sediment is fundamental to understanding its biogeochemical cycles, and ultimately its bioavailability and eutrophication potential to a lake ecosystem [28]. The ability to predict the occurrence and composition of eutrophic events, like harmful algal

blooms, has largely been inhibited by the lack of knowledge and understanding of the interactions that occur between nutrient enrichment and key physical, chemical, and biological characteristics of receiving waters [8].

There are several methods in which the phosphorus composition within lake sediment can be analyzed, including total phosphorus and sequential extractions of solid organic phosphorus. Although total phosphorus assays provide useful information, sequential extractions can better evaluate the fractionations and relative bioavailability of sediment phosphorus [36–39]. Five fractionations are used to characterize the phosphorus composition in terms of how tightly bound the phosphorus is to the solid phase, as determined by chemical solubility through increasingly stronger acidic or basic treatments to the sediment [34,40,41]. In order of increasing solid phase affinity, these fractionations are loosely-bound or “exchangeable”, iron-bound, aluminum-bound, aluminum-bound + labile organic, and mineral-bound phosphorus [42]. However, neither of these two methods are capable of separating specific phosphorus compounds, and thus not able to clearly identify the phosphorus composition in the sediment.

The purpose of this project was to identify and characterize the phosphorus composition in sediment samples from various locations in Lake Superior and the St. Louis River Estuary using a sodium hydroxide-ethylenediaminetetraacetic acid (NaOH-EDTA) phosphorus extraction and  $^{31}\text{P}$  nuclear magnetic resonance ( $^{31}\text{P}$  NMR) spectroscopy. Identification of phosphorous composition would enable predictive modeling of internal loading levels given modification in lake conditions, such as water temperature, pH, or pollutant levels.

# METHODS

## SEDIMENT EXTRACTION PROCEDURE

Prior to extraction, sediment core samples were prepared at LLO by Dr. Robert Sterner's research group. On board the Blue Heron research vessel, sediment cores were sliced into 1 or 5 cm segments and bagged separately. Samples were then frozen prior to drying. Using a mortar and pestle, samples were ground into a powdery consistency, then stored prior to analysis.

For solution  $^{31}\text{P}$  NMR, first an extraction must be performed on the ground samples produced from the sediment core preparation procedure above. Several extraction procedures used in previous studies have included NaOH [43,44], Chelex in water [45,46], NaOH in addition to Chelex [47], NaOH and sodium fluoride [48], and NaOH plus EDTA [49–51]. This investigation focused on phosphorus extraction using NaOH and EDTA. Although EDTA and Chelex help release phosphorus from paramagnetic ions, Chelex has been known to also remove polyphosphate compounds [47,48,50]. Furthermore, EDTA has been shown to extract more phosphorus than Chelex; however, iron and magnesium remain in solution [50,52], which may increase line broadening in the  $^{31}\text{P}$  NMR spectra due to the presence of these paramagnetic ions.

Using a modified NaOH-EDTA extraction [50,53], 11 sediment samples (six from Lake Superior and five from the St. Louis River Estuary) were extracted in the following procedure. Approximately 5 grams of processed dry sediment was weighed out and placed into a 50-mL conical centrifuge tube, to which 20 mL of 0.5 M NaOH and 20 mL 0.1 M EDTA was added. Using a shaker tray, tubes were agitated for a minimum of 12

hours. Shaker speed was varied because sample resuspension varied between samples. Care was taken to ensure the sediment remained suspended while simultaneously avoiding any spills. Samples were then centrifuged at 30,000 RPM for 30 minutes and the supernatant was removed and placed into a second 50-mL conical centrifuge tube and placed into a -80°C freezer until frozen. Lastly, the solvent was removed via freeze-drying samples and the dried material was kept in a refrigerator (2°C) until NMR tube preparation.

### <sup>31</sup>P NMR PREPARATION

Hydrolysis of phosphorus samples is a known issue [50,54,55] and needs to be minimized or avoided as much as possible. Keeping total experimental time as short as possible is the best way to avoid hydrolysis [56]; therefore, all samples were analyzed within three days of NMR tubes preparation. Approximately 200-300g of the freeze-dried extract was weighed into an acid-washed glass vial. A 9:1 solution of 1.0M NaOH and deuterium oxide (D<sub>2</sub>O; solvent lock) was used to re-dissolve the extracts. The addition of NaOH increased the pH of the solution to above 12, resulting in the deprotonation of compounds. This ensured consistent chemical shifts and spectral resolution [53]. To avoid diluting the phosphorus signal too much, the solvent was added drop-wise until no large particles were visible. Any remaining particles were filtered out prior to transfer into 5mm NMR (7 inch WILMAD 528) tubes using glass wool and a glass pipette.

### <sup>31</sup>P NMR ACQUISITION PROTOCOL

<sup>31</sup>P NMR analysis was performed at the University of Minnesota Twin Cities Department of Chemistry's Nuclear Magnetic Resonance Laboratory under the supervision of Dr.



Letitia Yao [57]. Spectra were collected using a Bruker Avance III 500 spectrometer, operating at 203MHz with a 5mm BBFO "SmartProbe" with z-axis gradients. Initial  $^{31}\text{P}$  NMR experiments were performed to determine the specific parameters that best fit the samples studied within this investigation. Sample CB12 was used for parameter adjustments so that spectral consistency was maintained for comparative analysis.

The default phosphorus data acquisition sequence without proton decoupling supplied by Bruker was used as a starting basis for initial  $^{31}\text{P}$  NMR experimental set-up. Proton decoupling was not utilized in this project, even though it is commonly accepted to do so. The decision to not pursue proton decoupling was due to concerns around the radio frequency (RF) power heating the sample itself, making it difficult to control the temperature with the NMR spectrometer temperature control unit [58,59]. Additionally, Cade-Menun and Liu [56] concluded that proton decoupling is less necessary for  $^{31}\text{P}$  NMR analysis compared to  $^{14}\text{C}$  NMR analysis since the phosphorus-proton couplings are separated by two or more bonds. This results in less peak splitting than what is often observed in carbon-proton single bond splitting patterns.

The default Bruker  $^{31}\text{P}$  NMR analysis used a  $30^\circ$  pulse angle with a 3.24 second acquisition time and a 2.00 second pulse delay. Spectra were initially collected at 300, 1000, 5000, and 7500 scans to confirm that resolution and signal-to-noise (S/N) ratio would be improved with increasing number of scans. Secondary adjustments to the default  $^{31}\text{P}$  NMR acquisition sequence held the number of scans at 5000 to investigate the significance of acquisition time, pulse delay time, and pulse width. The ranges under investigation were 1.99 to 3.24 seconds, 1.00 to 2.00 seconds, and  $30^\circ$  to  $90^\circ$ , respectively. Instrument availability allowed for an increased number of collection scans.

## RESULTS AND DISCUSSION

### <sup>31</sup>P NMR OPTIMIZATION STUDY

Initial optimization for <sup>31</sup>P NMR acquisition protocol was determining number of scans required to achieve good resolution and S/N ratio. Figure 5 shows a spectral overlay of increasing number of scans. As evident, the resolution and S/N ratio improve as the number of scans increases from 300 to 7500. This trend was expected to be maintained, and therefore, the final number of scans used for analysis was 9000 based on having additional instrument time available.

Secondary optimization adjusted other parameters to further improve resolution and S/N ratio, as well as decrease the risk of hydrolysis. Regarding acquisition time and pulse delay time, many references report an acquisition time ranging between 0.1 and 1.99 seconds, and delay times ranging between 0.2 and 30 seconds (see Table 5 in [56]). The summation of acquisition time and pulse delay time is the total acquisition time (AQ/D1) and it determines the total NMR analysis time. The default <sup>31</sup>P NMR protocol had an AQ/D1 of approximately 5 seconds, which resulted in one experimental run of 9000 scans to last over 13 hours. As stated previously, decreasing the overall experimental time helps decrease the risk of hydrolysis; therefore, it was of interest to investigate if a shorter AQ/D1 time would affect the overall spectral results. Sample CB12 was analyzed at AQ/D1 values of 3 and 5 seconds, as shown in Figure 6. Aside from a small disturbance around 6 ppm, which can be attributed to the asymmetry of the two large peaks due to shouldering, there is no difference between the two AQ/D1 values, as shown in the top spectral difference line in Figure 6. Since the quality of the spectrum

was maintained, samples were able to be analyzed at an AQ/D1 of 3 seconds, which reduced experimental time to 7.5 hours for 9000 scans, further reducing the risk of hydrolysis.

It should be noted that for quantitative analysis, the pulse delay must be long enough to allow for complete relaxation of phosphorus. To achieve this, it requires the determination of the longest  $T_1$  value within their sample.  $T_1$  relaxation corresponds to the process of establishing (or re-establishing) the normal Gaussian population distribution of  $\alpha$  and  $\beta$  spin states in the magnetic field [60]. It is the process by which the net magnetization grows or returns to its initial maximum value, parallel to the applied magnetic field [61]. According to Cade-Menun *et al.*, 1-2 seconds is adequate for most environmental samples, but a general rule for delay time is three to five times the  $T_1$  value for quantitative analysis. Depending on the pulse angle; this will allow for a 99.3% return to equilibrium [62–64].

For pulse width determination, although a 30°-pulse width would result in the shortest pulse delay time and allow for a quicker pulse rate, the disadvantage is reduced signal per pulse [56], whereas 90°-pulse width provides the maximum signal per pulse. This is illustrated in Figure 7. The bottom spectral line, which corresponds to a 30°-pulse width, has less separation between neighboring peaks located around 5 ppm as compared to the 90°-pulse width.

The  $^{31}\text{P}$  NMR protocol parameters selected for the remainder of this investigation were 9000 scans, 90° pulse width, 1.99 second acquisition time, and 1.00 second delay time. Additionally, post peak processing consisted of 10Hz line-broadening to eliminate splitting due to analyzing without proton decoupling [55].

## SPECTRAL RESULTS AND DISCUSSION

Lake Superior sediment samples (CB3, CB4, CB10, CB11, CB12) and St. Louis River Estuary samples (SLRE2, SLRE5, SLRE6, SLRE9) were analyzed using the developed  $^{31}\text{P}$  NMR protocol. Although sediment samples CB9 and SLRE10 underwent the phosphorus extraction procedure, ultimately, they were not analyzed via  $^{31}\text{P}$  NMR due to a visible amount of moisture remaining in the freeze-dried material. Due to following a specific sample preparation procedure [50], this investigation was able to use a peak library for environmental samples prepared by Cade-Menun for peak identification [50,55,63]; however, since an internal standard was not included to determine exact shifting differences due to systematic and random error, peaks cannot be identified with exact certainty. Therefore, compound identification will include all compounds with  $\pm 0.5$  ppm of the measured peak signal.

### *LAKE SUPERIOR CHEQUAMEGON BAY SEDIMENT SAMPLES*

Figure 8 shows the overlaid spectral results for CB samples. Sediment core depth effects on phosphorus composition have been previously studied, and showed a disappearance of phosphorus compounds, with pyrophosphate declining first, followed by phosphorus esters then orthophosphate as core depth increases; however, these effects were not seen to a great effect until sediment depths of 4-5 cm[65]. Recalling that samples CB3 and CB4 are the 0-1 cm and 1-2 cm samples, respectively, from the same core. Table 3 shows there is little difference between phosphorus composition between the two samples, which is consistent with results found by Ahlgren *et al.* [65], since spectral differences wouldn't be noticeable until core depths greater than 4 cm.

The spectral results for CB10 and CB11 are also of interest. As stated previously, these sediment samples and the extracted material were unlike the other samples in physical appearance. As evident in Figure 8, these two sites do not exhibit as varied of sediment phosphorus composition as the ones observed in the CB3, CB4, and CB12 samples.

Table 3 includes measured peaks and likely phosphorus compound identification for the Chequamegon Bay samples. There is a trend between water depth at sampling site and sediment phosphorus composition variation. Referring to Table 1, sample site depths vary between all of the samples with CB10 being the shallowest sample site and CB3/4 being the deepest sample site. As the water depth at the sample site increases, more phosphorus compound groups start to appear in the  $^{31}\text{P}$  NMR spectra. Similarly, this trend is also present in the sequential phosphorus fractionation results (Figure 9) for the same sediment samples. This correlation between increasing water depth and increasing number of peaks is summarized in Table 3 and explained below.

The  $^{31}\text{P}$  NMR spectrum of the shallowest sample, CB10, shows a single peak at 5.41 ppm, and the fractionation profile indicates this compound exists in the mineral-bound and aluminum-bound phosphorus fractions. The next deepest sample, CB11, shows an addition of a second peak at 3.31 ppm. Similarly, the fractionation profile for CB11 shows the increase in relative abundance of the phosphorus detected in the aluminum-bound + labile organic fraction. Sample CB12 has a third peak at 1.94 ppm, as well as the increased presence of the iron-bound phosphorus in its fractionation profile. Lastly, the deepest samples, CB3 and CB4, which have very similar  $^{31}\text{P}$  NMR spectra, show the disappearance of the peak at 1.94 ppm, but show a different peak around -1.1

ppm. Additionally, there was the addition of a fourth peak around -5.0 ppm detected, as well as the addition of loosely-bound phosphorus in their fractionation profile. Polyphosphate and phosphonate were not detected in the spectra of any samples, the significance of which will be discussed later.

This association shows that sediment composition is dependent on factors associated with changing water depth. One factor could be the effective settling velocity at these locations. Sediment in shallow water is more likely to be affected by turbulent water conditions than sediment at deeper water depths. This prohibits the settling of suspended solids, to which phosphorus compounds adhere to, and could contribute to not detecting additional phosphorus compounds or fractionations until deeper depths have been reached.

#### *ST. LOUIS RIVER ESTUARY SEDIMENT SAMPLES*

Figure 9 shows the overlaid spectral results for SLRE samples. St. Louis River Estuary sediment samples showed similar spectral results as the Lake Superior sediment samples, with the exception of CB10. All four SLRE samples have peaks around 5.4 ppm, 4.0 ppm, and -1.1 ppm, and SLRE5 had another peak at -4.93 ppm. Peak identifications for SLRE samples are comparable to those identified in Table 3 for the Chequamegon Bay samples.

The resultant spectral profiles for the SLRE samples suggests that the phosphorus in sediment in the SLRE is responding to factors similar to those present in Lake Superior. These locations exhibit similar spectral results to Lake Superior results since the SLRE is essentially a sequence of increasingly larger pools that present the hydrodynamics of small lakes, which offer more opportunities for sedimentation to occur.

As the St. Louis River enters the first of the lakes in the SLRE by Station 2, a river-lake interface is present, where water velocity drastically reduces and the effective settling velocity of suspended particles increases. This continues throughout the SLRE until the water reaches the estuary-lake interface leading into Lake Superior, where final sedimentation will primarily occur.

## LITERATURE COMPARISONS

$^{31}\text{P}$  NMR studies have been performed on many lakes across the globe. The sediment samples from Lake Superior near Chequamegon Bay and from the SLRE are consistent with other lakes studied. In general, a range of compounds containing phosphorus were found, including orthophosphate (inorganic and organic), orthophosphate monoesters and diesters, pyrophosphate, polyphosphate, and phosphonate [66–71].

As stated previously, none of the samples analyzed in this study detected the presence of polyphosphate or phosphonate. Using  $^{31}\text{P}$  NMR, Hupfer and Gächter reported polyphosphate peaks (-19 to -21 ppm [43,44,50]) in surface sediment sample samples from Lake Baldegg and Lake Lucern, eutrophic and oligo-mesotrophic lakes, respectively[70]. Similarly, in particulate samples from the eutrophic Lake Mendota,  $^{31}\text{P}$  NMR analysis also detected polyphosphates (-19 to -21 ppm [43,44,50]) and phosphonates (20 ppm [43,44,50]). Polyphosphates are common in fertilizers and phosphonates are common herbicides, they are found in sediment near high agricultural runoff areas, where eutrophic lakes are commonly found. Therefore, the lack of these two compounds aligns with the assertion that Lake Superior is an oligotrophic waterbody. Additionally, this suggests that as the trophic status of a lake progresses from oligotrophic to eutrophic, the phosphorus composition of the sediment also differs,

suggesting that the presence of polyphosphates and phosphonates in the sediment could be a strong indicator for determining the trophic status of a waterbody.

## CONCLUSIONS

As stated before, understanding the specific chemical composition of phosphorus in sediment is fundamental to understanding its bioavailability and eutrophication potential to a lake ecosystem.  $^{31}\text{P}$  NMR spectroscopy provides a more direct characterization of the distribution of phosphorus in sediment, and will allow the ability to better predict the sediment retention fluxes of particulate phosphorus. Gaining an understanding of these fluxes will help produce a model that can predict changes in phosphorus cycling in the event hydrological conditions change measurably.

A working alkaline extraction and  $^{31}\text{P}$  NMR acquisition procedure were developed and used to analyze the phosphorus composition at several sites within Lake Superior near Chequamegon Bay and the SLRE. Chequamegon Bay samples (CB3, CB4, CB10, CB11, and CB12) showed an association between increasing sediment phosphorus variations with increasing water depth, which was similarly observed in fractionation data. Samples from the SLRE exhibit similar phosphorus composition to the CB samples (with the exception of CB10), suggesting that the small pools within the estuary mimic the relative change in hydrological conditions like those at the mouth of the river entering Lake Superior near Chequamegon Bay. Resulting spectra confirmed that samples from Lake Superior near Chequamegon Bay and SLRE sediments contained typical



phosphorus compounds in comparison to sediment analyses from other, previously studied oligotrophic waterbodies.

Aligning with the understanding that Lake Superior is an oligotrophic waterbody, the most abundant peak for all samples was detected around 5.4 ppm. Although the exact identification of this peak cannot be confirmed due to the lack of an internal standard, it is highly likely that this peak is inorganic orthophosphate. As stated before, Lake Superior has a high oxygen penetration into the sediment, measured as deep as 12 cm, resulting in low solubility for ferric hydroxide compounds to which inorganic phosphates adsorb, creating a phosphorus sink within the sediment [19,20].

Further supporting the principle that Lake Superior is an oligotrophic waterbody, this analysis did not detect the presence of polyphosphate or phosphonate, two compounds that have been detected in lakes with a higher level of primary productivity. The presence or lack of presence of polyphosphate and phosphonate in  $^{31}\text{P}$  NMR analysis could be used as a method to monitor the trophic status of a waterbody. This could be employed across an entire waterbody, or could be focused on the edges of eutrophic sections of a lake to predict future areas of concern.

## FUTURE WORK

A useable phosphorus extraction procedure and working a  $^{31}\text{P}$  NMR acquisition sequence were determined and utilized, which were the two major goals for this investigation. Nevertheless, there are ample opportunities to expand on the work done so that greater

understanding of sediment-water interactions, specifically as they relate to phosphorus cycling, can be achieved.

The first opportunity for future work would be to confirm peak shifting ranges with an internal standard. This will confirm the identity of the peaks detected and could be used in conjunction with quantitative analysis, which would require the determination of the longest  $T_1$  relaxation time in the sample.

A second opportunity would be to continue analyzing sediment samples as described herein across more areas of Lake Superior and the SLRE to produce a complete geochemical profile of sediment phosphorus composition. Sediment sample analysis farther upstream in the St. Louis River would aid in establishing where and when phosphorus composition in sediment is determined. Additionally, analysis of sediment in proximity to the exit of the estuary and harbor would help connect estuary sample trends to deep-water trends.

In conjunction with analysis across Lake Superior and within the SLRE, the data could be used to build sediment-phosphorus transport and baseline models. Developing a transport dynamic model could be used to determine how phosphorus changes across the lake floor, as well as if there are unique zones within the lake. Additionally, since Lake Superior is still considered oligotrophic, a comprehensive sediment analysis would provide a baseline for current conditions. This baseline model could be used to predict the extent of internal loading of phosphorus into the water column under given hydrological changes, as well as be used as a benchmark to compare phosphorus sediment changes overtime.

Another opportunity would be combining sequential extraction fractionation with  $^{31}\text{P}$  NMR analysis. Fractionation investigations are relatively simple to perform; however, their results should be read with caution, especially in reference to organic phosphorus. As discussed by Turner *et al.*, specific groups of compounds are likely present in more than one fraction and bioavailable fractions are specific to the area from which the sample is taken [54]. Additionally, un-extractable fractions are assumed to be organic phosphorus, yet there exists no direct evidence to support this conclusion [54]. Separate  $^{31}\text{P}$  NMR analysis of each fraction from the sequential extraction procedure would clearly identify the phosphorus composition and assist in modeling the bioavailability of phosphorus from internal loading.

## ILLUSTRATIONS



*Figure 1: Lake Erie algal bloom captured on July 28, 2015 by the Operational Land Imager on Landsat 8. (Image courteous of NASA)*



*Figure 2: Aerial view of Lake Superior with sampling sites shown in boxes. Lake Superior CB sample location is outlined in blue and SLRE sample location is outlined in yellow See Figures 3 and 4, respectively, for more detail.*

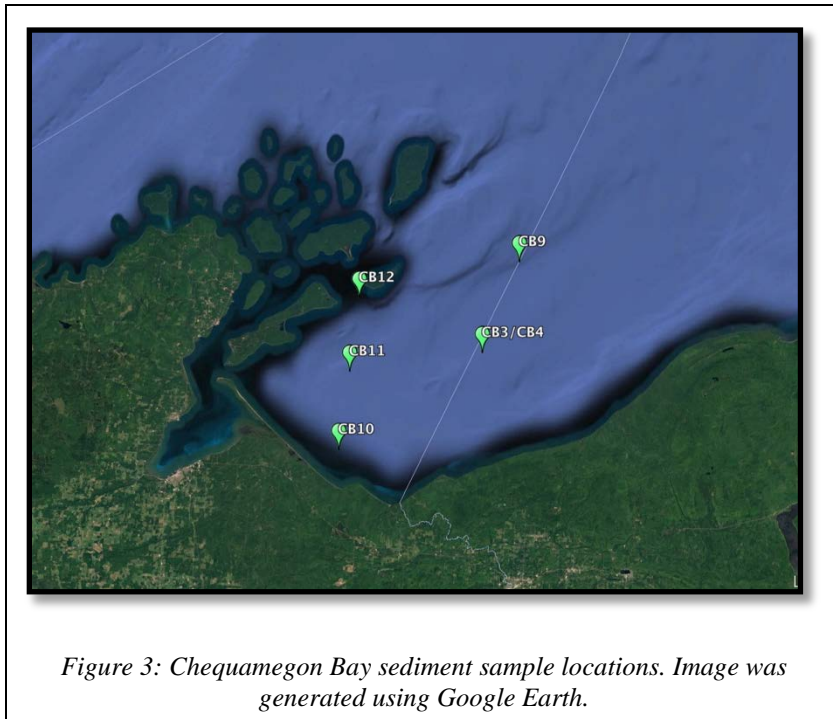


*Table 1: Water depths for Chequamegon Bay sampling locations.*

Station	Water Depth (m)
CB 3	15-17
CB 4	15-17
CB 9	23-25
CB 10	1-3
CB 11	3-5
CB 12	4-6

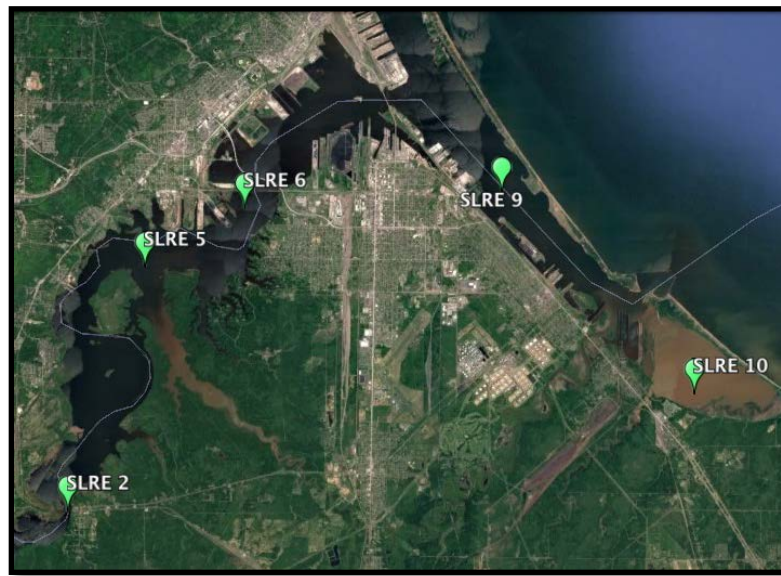


*Figure 4: St. Louis River Estuary sediment sample locations. Image generated using Google Earth.*

*Table 2: Water depths for St. Louis River Estuary sample sites.*

Station	Water Depth (m)
SLRE 2	1
SLRE 5	3
SLRE 6	2
SLRE 9	2.5
SLRE 10	2.5

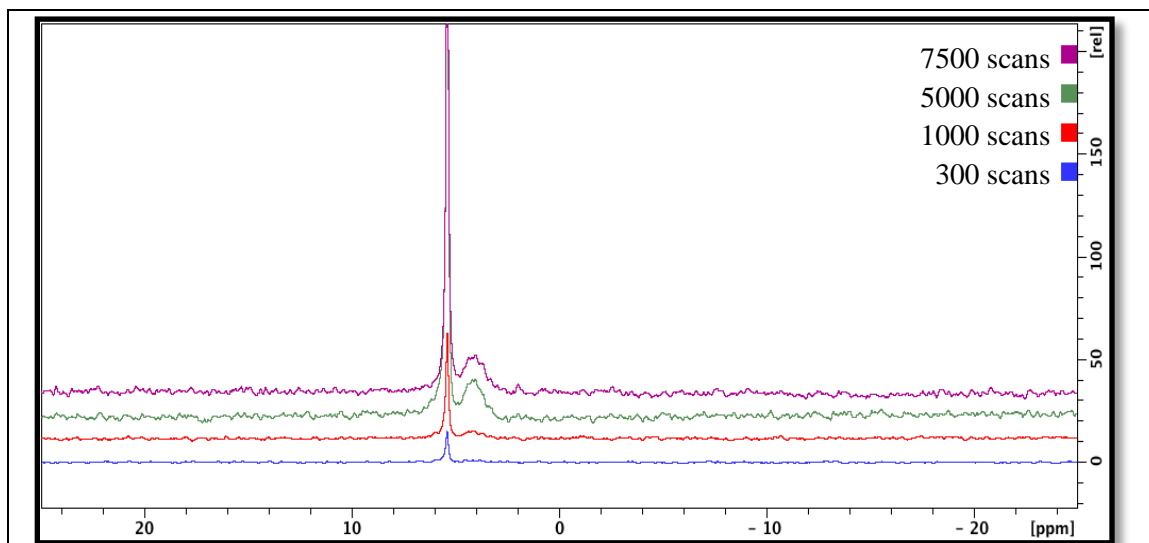


Figure 5: Sample CB12 collected with Bruker default  $^{31}\text{P}$  NMR protocol with increasing number of scans. As the number of scans increased, the spectral resolution also increased.

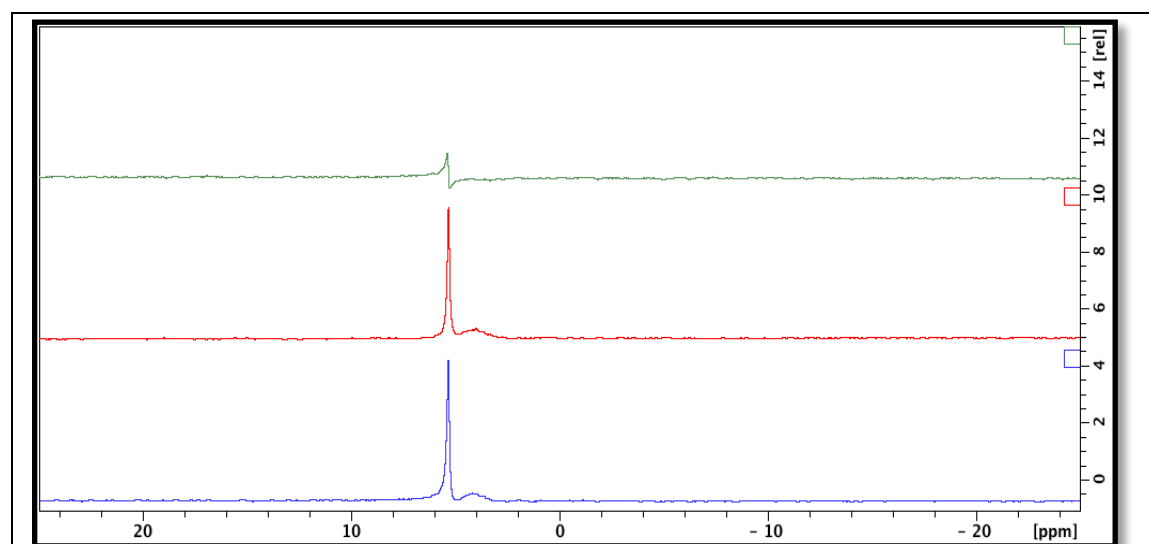
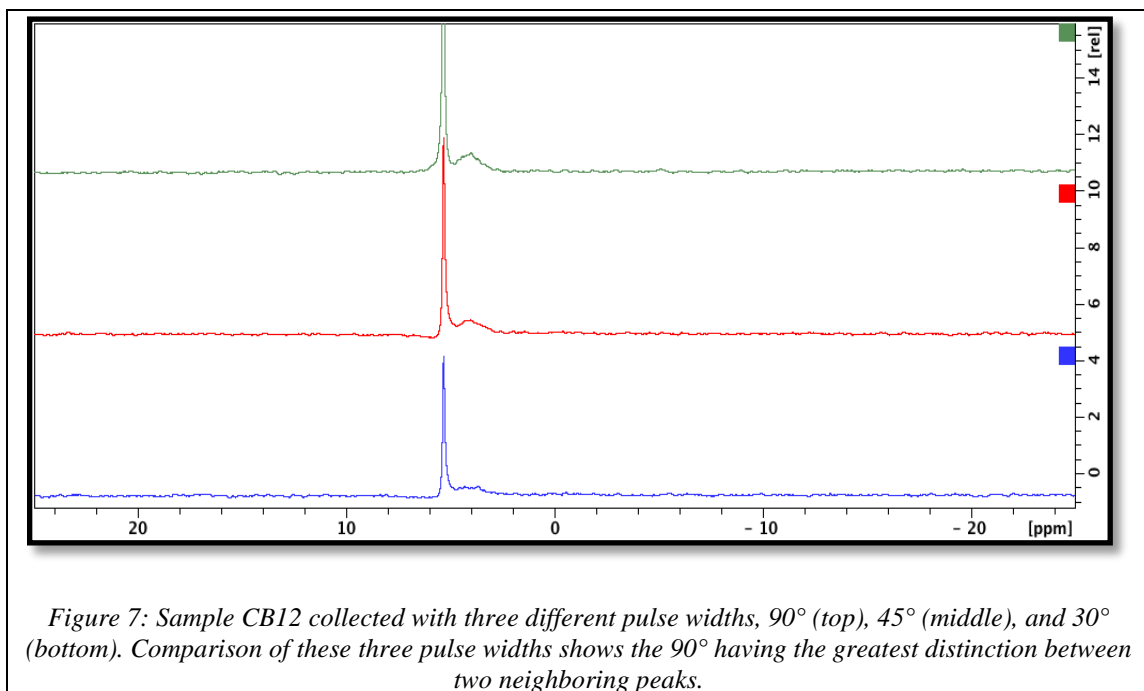


Figure 6: Sample CB12 collected at 90° pulse width for 5000 scans for AQ/D1 of 3 seconds (middle) and AQ/D1 of 5 seconds (bottom), with spectral difference between the two displayed on top.





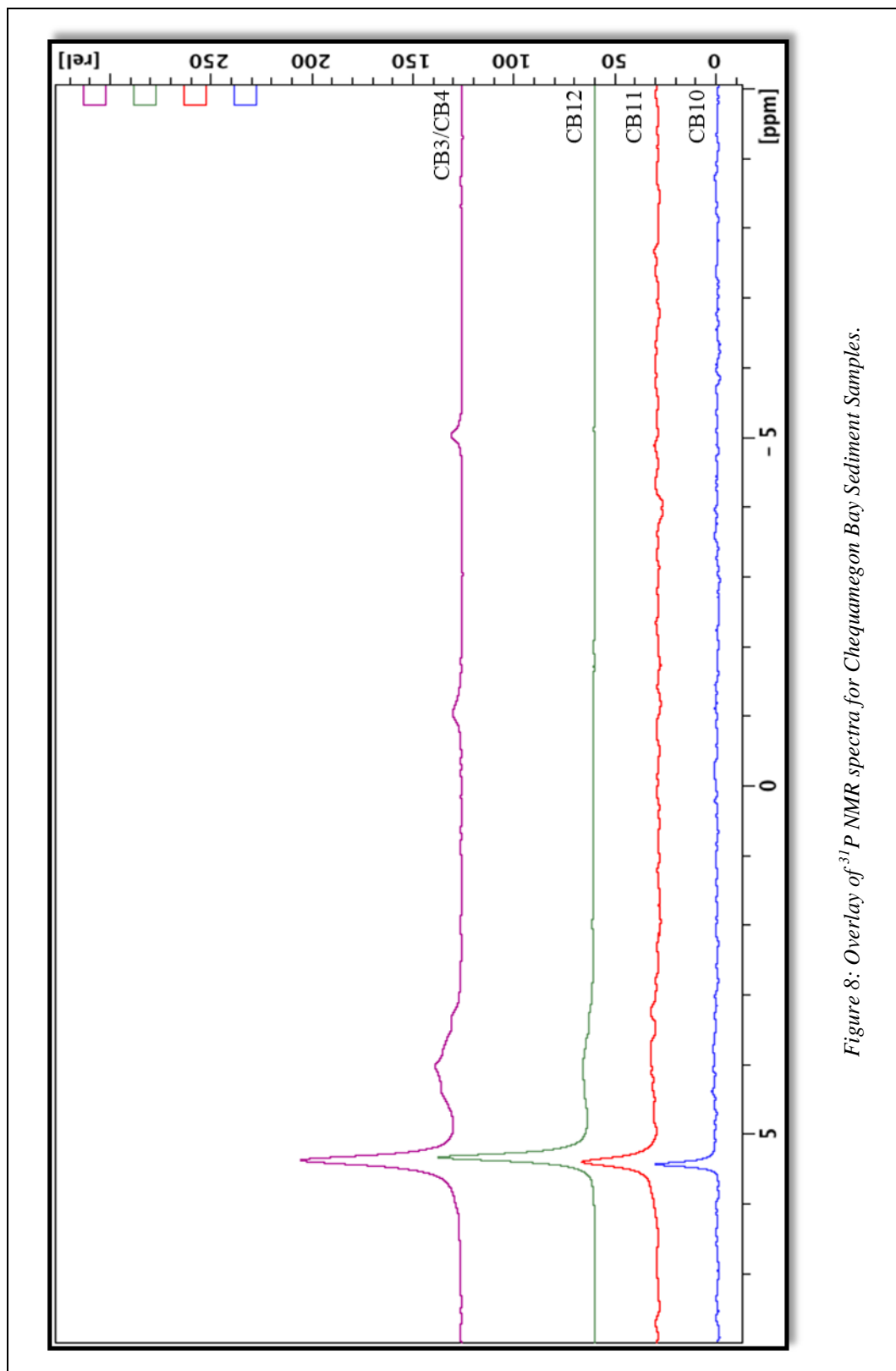


Figure 8: Overlay of  $^{31}\text{P}$  NMR spectra for Chequamegon Bay Sediment Samples.

Table 3: Chequamegon Bay phosphorus compound identification based on  $\pm 0.5$  ppm from measured NMR peak.

Sample	Measured Peak [ppm]	Peak Identification[55,63,72,73]
CB10	5.41	Inorganic orthophosphate Orthophosphate Orthophosphate monoesters Glucose-6-phosphate
CB11	5.44 3.31	Inorganic orthophosphate Orthophosphate Orthophosphate monoesters Glucose-6-phosphate Orthophosphate monoesters Glucose-1-phosphate
CB12	5.31 3.98 1.94	Inorganic orthophosphate Orthophosphate Orthophosphate monoesters Glucose-6-phosphate $\beta$ -glycerophosphate Glucose-1-phosphate Choline phosphate Scyllo-inositol hexakisphosphate Phosphate monoesters Orthophosphate diesters Teichoic acids Phosphatidyl ethanolamine Phosphatidyl serine Phosphate monoesters Nucleic acids
CB3/CB4	5.36/5.35 4.00/4.01 -1.10/-1.07 -5.02/-5.05	Inorganic orthophosphate Orthophosphate Orthophosphate monoesters Glucose-6-phosphate $\beta$ -glycerophosphate Orthophosphate monoesters Phytic acid Mononucleotides Scyllo-inositol hexakisphosphate Choline phosphate Orthophosphate diesters Phosphate end groups/ATP Pyrophosphate

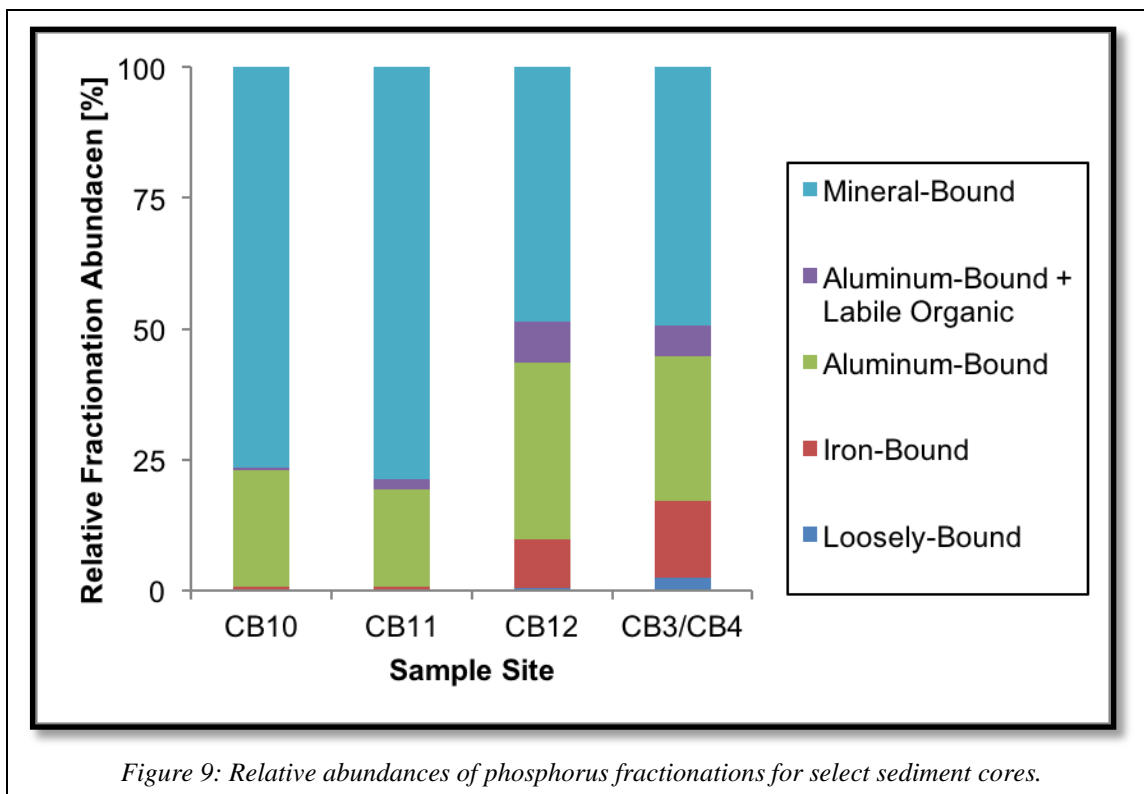


Figure 9: Relative abundances of phosphorus fractionations for select sediment cores.

Table 4: Summary of observed  $^{31}\text{P}$  NMR peaks for CB samples compared to site depth.

Location (Depth)	Peaks Observed [ppm]				
CB10 (1-3 m)	5.41	-	-	-	-
CB11(3-5 m)	5.44	3.31	-	-	-
CB12 (4-6 m)	5.31	3.98	1.94	-	-
CB3 (15-17 m)	5.36	4.00	-	-1.10	-5.02
CB4 (15-17 m)	5.35	4.01	-	-1.07	-5.05

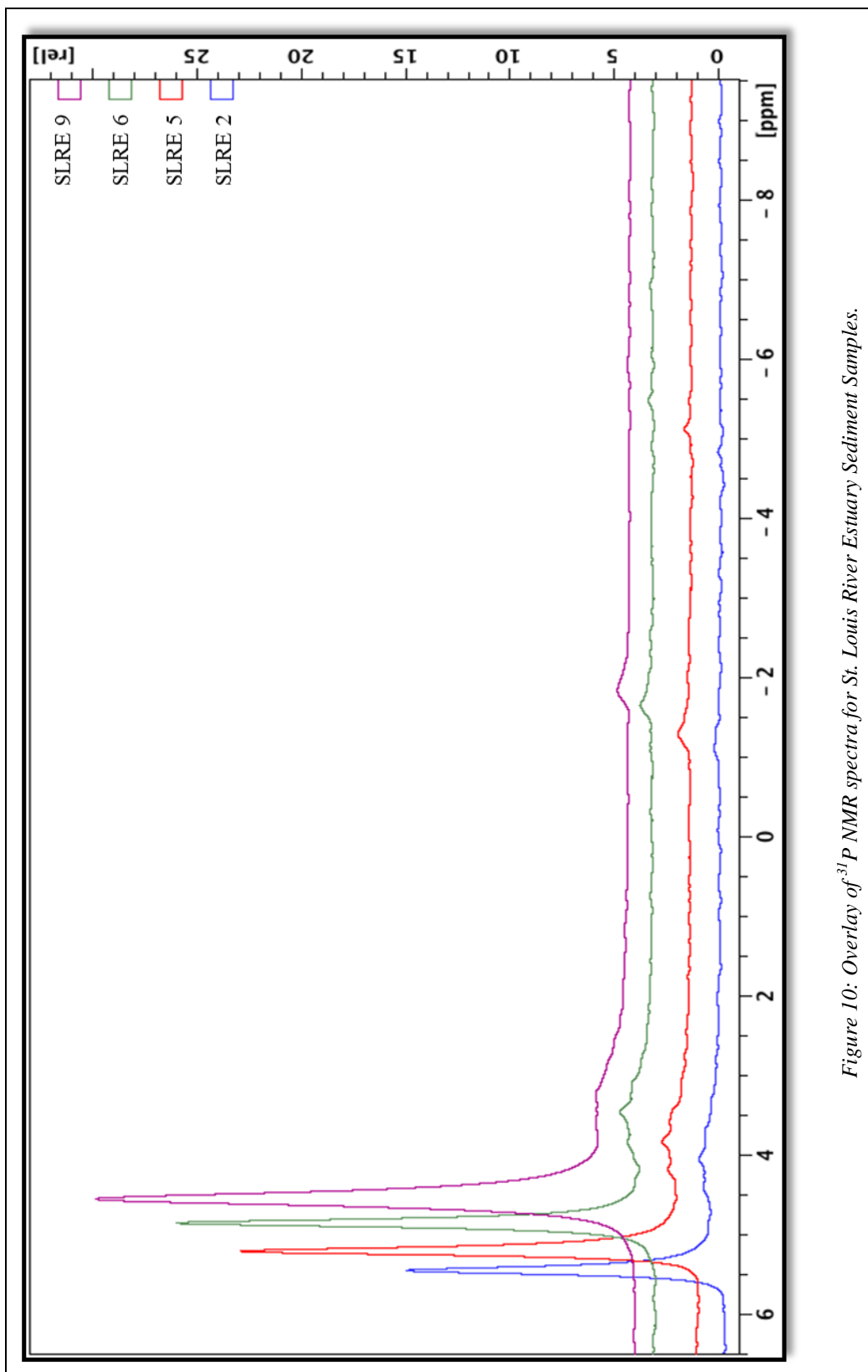


Figure 10: Overlay of  $^{31}\text{P}$  NMR spectra for St. Louis River Estuary Sediment Samples.

## BIBLIOGRAPHY

- [1] D.A. Chin, *Water-Quality Engineering in Natural Systems*, Second, Wiley, 2013.
- [2] K.D. McMahon, E.K. Read, *Annu. Rev. Microbiol.* 67 (2013) 199–219.
- [3] S. Katsev, (2016) 115–132.
- [4] R.E. Hecky, P. Kilham, *Limnol. Oceanogr.* 33 (1988) 796–822.
- [5] D.E. Schindler, S.R. Carpenter, J.J. Cole, J.F. Kitchell, M.L. Pace, *Science* (80-. ). 277 (1997) 248–251.
- [6] V.H. Smith, G.D. Tilman, J.C. Nekola, *Environ. Pollut.* 100 (1998) 179–196.
- [7] R. Gachter, S.M. Steingruber, M. Reinhardt, B. Wehrli, *Aquat. Sci.* 66 (2004) 117–122.
- [8] V.H. Smith, D.W. Schindler, *Trends Ecol. Evol.* 24 (2009) 201–207.
- [9] X. Jin, S. Wang, Y. Pang, H. Zhao, X. Zhou, *Colloids Surfaces A Physicochem. Eng. Asp.* 254 (2005) 241–248.
- [10] R.W. Howarth, in: *Pew Ocean. Comm.*, 2002.
- [11] V. Smith, *Environ. Sci. Pollut. Res.* 10 (2003) 126–139.
- [12] M. Søndergaard, J.P. Jensen, E. Jeppesen, *Hydrobiologia* 506–509 (2003) 135–145.
- [13] T. Young, J. V. DePinto, L.M. Meilroy, *Environ. Sci. Technol.* 20 (1978) 752–759.
- [14] D.M. Dolan, S.C. Chapra, *J. Great Lakes Res.* 38 (2012) 730–740.
- [15] National Research Council, *Restoration of Aquatic Ecosystems*, 1992.
- [16] Great Lakes Water Quality Agreement Nutrient Annex Subcommittee, (2015) 1–8.
- [17] A.M. Michalak, E.J. Anderson, D. Beletsky, S. Boland, N.S. Bosch, T.B. Bridgeman, J.D. Chaffin, K. Cho, R. Confesor, I. Daloglu, J. V. DePinto, M.A. Evans, G.L. Fahnenstiel, L. He, J.C. Ho, L. Jenkins, T.H. Johengen, K.C. Kuo, E. Laporte, X. Liu, M.R. McWilliams, M.R. Moore, D.J. Posselt, R.P. Richards, D. Scavia, A.L. Steiner, E. Verhamme, D.M. Wright, M.A. Zagorski, *Proc. Natl. Acad. Sci. U. S. A.* 110 (2013) 6448–52.
- [18] Raj Bejankiwar, in: *Counc. Gt. Lakes Ind.*, 2014, p. 100.
- [19] E.A. Heinen, J. McManus, *J. Great Lakes Res.* 30 (2004) 113–132.
- [20] J.Y. Li, S.A. Crowe, D. Miklesh, M. Kistner, D.E. Canfield, S. Katsev, *Limnol. Oceanogr.* 57 (2012) 1634–1650.
- [21] Wisconsin Department of Natural Resources, (2012).
- [22] M. Søndergaard, J.P. Jensen, E. Jeppesen, *Hydrobiologia* 408/409 (1999) 145–152.
- [23] J. Austin, S.M. Colman, *Limnol. Oceanogr.* 53 (2008) 2724–2730.
- [24] J. Austin, S.M. Colman, *Geophys. Res. Lett.* 34 (2007) 1–5.
- [25] K. Van Cleave, J.D. Lenters, J. Wang, E.M. Verhamme, *Limnol. Oceanogr.* 59 (2014) 1889–1898.
- [26] T.S. Hebner, S. Brovold, A. Ajanic, R. Sterner, E.M. Hill, G.H. Merten, in: *Minnesota Water Resour. Conf.*, 2016.

- [27] Y. Zhu, F. Wu, Z. He, J.P. Giesy, W. Feng, Y. Mu, C. Feng, X. Zhao, H. Liao, Z. Tang, *Chem. Geol.* 397 (2015) 51–60.
- [28] Y. Zhu, R. Zhang, F. Wu, X. Qu, F. Xie, Z. Fu, *Environ. Earth Sci.* 68 (2013) 1041–1052.
- [29] Y. Zhu, F. Wu, Z. He, J. Guo, X. Qu, F. Xie, J.P. Giesy, H. Liao, F. Guo, *Environ. Sci. Technol.* 47 (2013) 7679–7687.
- [30] W. Granéli, *Hydrobiologia* 404 (1999) 19–26.
- [31] W. Scharf, *Hydrobiologia* 416 (1999) 85–96.
- [32] K. Fytianos, A. Kotzakioti, *Environ. Monit. Assess.* 100 (2005) 191–200.
- [33] Y.Q. Fu, Y.Y. Zhou, J.Q. Li, *J. Environ. Sci.* 12 (2000) 57–62.
- [34] K.C. Ruttenger, *Limnol. Oceanogr.* 37 (1992) 1460–1482.
- [35] A.N. Balchand, S.M. Nair, *Environ. Geol.* 23 (1994) 284–294.
- [36] Q. Zhou, C.E. Gibson, Y. Zhu, *Chemosphere* 42 (2000) 221–225.
- [37] H.L. Golterman, *Limnetica* 20 (2001) 15–29.
- [38] D.C. Ribeiro, G. Martins, R. Nogueira, J. V. Cruz, A.G. Brito, *Chemosphere* 70 (2008) 1256–1263.
- [39] Z. Ai-min, W. Dong-sheng, T. Hong-xiao, *J. Environ. Sci. (IOS Press)* 17 (2005) 384–388.
- [40] A.M. Abdel-Satar, M.F. Sayed, *Environ. Monit. Assess.* 169 (2010) 169–178.
- [41] B.L. Turner, A.B. Leytem, *Environ. Sci. Technol.* 38 (2004) 6101–6108.
- [42] S. Brovold, G.H. Merten, T.S. Hebner, A. Ajanic, (2016).
- [43] R.H. Newman, K.R. Tate, *Commun. Soil Sci. Plant Anal.* 11 (1980) 835–842.
- [44] G.E. Hawkes, D.S. Powlson, E.W. Randall, K.R. Tate, *J. Soil Sci.* 35 (1984) 35–45.
- [45] M.A. Adams, L.T. Byrne, *Soil Biol. Biochem.* 21 (1989) 523–528.
- [46] L.M. Condon, I.S. Cornforth, M. Davis, R.H. Newman, *Biol. Fertil. Soils* 21 (1996) 37–42.
- [47] N. Gressel, J.G. McColl, C.M. Preston, R.H. Newman, R.F. Powers, *Biogeochemistry* 33 (1996) 97–123.
- [48] M. Sumann, W. Amelung, L. Haumaier, W. Zech, *Soil Sci. Soc. Am. J.* 62 (1998) 1580.
- [49] B.L. Turner, N. Mahieu, L.M. Condon, *Soil Sci. Soc. Am. J.* 67 (2003) 497–510.
- [50] B.J. Cade-Menun, C.M. Preston, *Soil Sci.* 161 (1996) 770–785.
- [51] R.A. Bowman, J.O. Moir, *Soil Sci. Soc. Am. J.* 58 (1993) 1516–1518.
- [52] K.R. Tate, G.J. Churchman, *Soil Biol. Biochem.* 14 (1982) 191–196.
- [53] B.L. Turner, R. Baxter, N. Mahieu, S. Sjögersten, B.A. Whitton, *Soil Biol. Biochem.* 36 (2004) 815–823.
- [54] B.L. Turner, B.J. Cade-Menun, L.M. Condon, S. Newman, *Talanta* 66 (2005) 294–306.
- [55] B.J. Cade-Menun, *Geoderma* 257–258 (2015) 102–114.
- [56] B.J. Cade-Menun, C.W. Liu, *Soil Sci. Soc. Am. J.* 78 (2014) 19–37.
- [57] L. Yao, UMN Chem. Dep. (2016) <http://nmr.chem.umn.edu/>.
- [58] J. Keeler, *Understanding NMR Spectroscopy*, 2005.

- [59] T.D.W. Claridge, *High-Resolution NMR Techniques in Organic Chemistry*, 2009.
- [60] H.J. Reich, (2010) 1–11.
- [61] AD Elster, *MRI Quest*. (2017).
- [62] B.J. Cade-Menun, C.W. Liu, R. Nunlist, J.G. McColl, *J. Environ. Qual.* 31 (2002) 457–465.
- [63] B.J. Cade-Menun, *Talanta* 66 (2005) 359–371.
- [64] D. Canet, *Nuclear Magnetic Resonance: Concepts and Methods*, 1996.
- [65] J. Ahlgren, L. Tranvik, A. Gogoll, M. Waldebäck, K. Markides, E. Rydin, *Environ. Sci. Technol.* 39 (2005) 867–872.
- [66] R. Carman, G. Edlund, C. Damberg, *Chem. Geol.* 163 (2000) 101–114.
- [67] D.S. Baldwin, *Hydrobiologia* 335 (1996) 63–73.
- [68] A. Khoshmanesh, B.T. Hart, A. Duncan, R. Beckett, 36 (2002) 774–778.
- [69] U. Selig, T. Hübener, M. Michalik, *Aquat. Sci.* 64 (2002) 97–105.
- [70] M. Hupfer, R. Gtichter, R.R. Ruegger, *Limnol. Oceanogr.* 40 (1995) 610–617.
- [71] M. Hupfer, B. Rube, P. Schmieder, *Limnol. Oceanogr.* 49 (2004) 1–10.
- [72] B.L. Turner, N. Mahieu, L.M. Condron, *Org. Geochem.* 34 (2003) 1199–1210.
- [73] C.N. Bedrock, M. V. Cheshire, J.A. Chudek, B.A. Goodman, C.A. Shand, *Sci. Total Environ.* 152 (1994) 1–8.
- [74] Office of Coast Survey, [Noaa.gov](http://Noaa.gov) (2017).